BJ www.biochemj.org

BJ Disease

Biochem. J. (2010) **431**, 363–371 (Printed in Great Britain) doi:10.1042/BJ20100668

A novel TMPRSS6 mutation that prevents protease auto-activation causes IRIDA

Sandro ALTAMURA*†, Flavia D'ALESSIO*†‡, Barbara SELLE§[1] and Martina U. MUCKENTHALER*†[1,2]

*Department of Pediatric Oncology, Haematology and Immunology, University Hospital of Heidelberg, Im Neuenheimer Feld 156, Heidelberg 69120, Germany, †Molecular Medicine Partnership Unit (MMPU), Im Neuenheimer Feld 153, Heidelberg 69210, Germany, ‡European Molecular Biology Laboratory (EMBL), Meyerhofstrasse 1, Heidelberg 69117, Germany, and §Helios Klinikum, Wiltbergstrasse 50, Berlin 13125, Germany

IRIDA (iron-refractory iron-deficiency anaemia) is a rare autosomal-recessive disorder hallmarked by hypochromic microcytic anaemia, low transferrin saturation and high levels of the iron-regulated hormone hepcidin. The disease is caused by mutations in the transmembrane serine protease *TMPRSS6* (transmembrane protease serine 6) that prevent inactivation of HJV (haemojuvelin), an activator of hepcidin transcription. In the present paper, we describe a patient with IRIDA who carries a novel mutation (Y141C) in the SEA domain of the *TMPRSS6* gene. Functional characterization of the TMPRSS6(Y141C) mutant protein in cultured cells showed that it localizes to similar subcellular compartments as wild-type TMPRSS6 and binds HJV, but fails to auto-catalytically activate itself. As a consequence, hepcidin mRNA expression is increased, causing the clinical symptoms observed in this IRIDA patient. The present study provides important mechanistic insight into how TMPRSS6 is activated.

Key words: haemojuvelin, hepcidin, iron-refractory iron-deficiency anaemia (IRIDA), matriptase-2, transmembrane protease serine 6 (TMPRSS6).

INTRODUCTION

Patients with IRIDA (iron-refractory iron-deficiency anaemia) absorb insufficient amounts of iron from the diet and respond inadequately to oral ferrous sulfate therapy and intramuscular iron dextran injection [1]. As a consequence of this iron deficiency, anaemia develops that is characterized by hypochromic microcytic erythrocytes and low transferrin saturation. IRIDA is usually diagnosed by routine haematological screening during childhood. Frequently, the affected subjects do not show the typical clinical symptoms of iron deficiency; pallor, dry skin or lesions at the corners of the mouth have been reported in only a few cases [2–4]. IRIDA is a rare autosomal-recessive disorder [5] mapped to chromosome 22 (22q12.3–13.2) [2], which contains *TMPRSS6* (transmembrane protease serine 6, also known as matriptase-2) the gene responsible for IRIDA [6]. *Tmprss6* was initially characterized in the *mask* mouse, in which chemically induced mutations resulted in the loss of the Tmprss6 protease domain. Similar to IRIDA patients and *Tmprss6*$^{-/-}$ mice [7], the mouse model is hallmarked by microcytic anaemia due to ineffective dietary iron absorption [8].

TMPRSS6 is a member of the TTSP (type II transmembrane serine protease) family and is mainly expressed in the liver [9]. Similar to other TTSP members, TMPRSS6 consists of a short N-terminal intracytoplasmic tail, a type II transmembrane domain, a stem region composed of two extracellular CUB [complement factor C1s/C1r, urchin embryonic growth factor and BMP (bone morphogenetic protein)] domains and three LDLR (low-density-lipoprotein receptor class A) domains and a C-terminal trypsin-like serine protease domain [9]. Between the transmembrane domain and the stem region there is a low homology SEA (sea urchin sperm protein, enteropeptidase and agrin) domain [10]. TMPRSS6 is rich in post-translational modifications. Consensus sites for N-glycosylation are located within the SEA domain, the second CUB domain and within the second LDLR domain [11]. A total of 37 evolutionarily conserved extracellular cysteine residues located within the CUB, the LDLR and the protease domains are at least partially involved in the formation of disulfide bridges [11]. *In silico* analysis of human TMPRSS6 revealed a possible phosphorylation site within the intracytoplasmic tail, which was hypothesized to be involved in signal transduction [9]. TMPRSS6 is produced as a zymogen, a single chain inactive proenzyme, which auto-activates itself by cleavage at an arginine residue at the consensus site RIVGG between the prodomain and the catalytic domain. The activated catalytic domain remains attached to the rest of the protein at the cell surface via a single disulfide bridge [9].

Functionally, TMPRSS6 has been linked to the hepatic iron-sensing pathway by the observation that hepcidin levels are strongly increased in IRIDA patients and *Tmprss6* mutant mice [2,6,8]. Hepcidin is a small peptide hormone produced by the liver in response to iron levels, inflammatory signals, hypoxia and the erythropoietic drive. Hepcidin controls systemic iron fluxes by binding to the iron exporter ferroportin, inducing its internalization and degradation [12]. Thus high hepcidin levels,

Abbreviations used: ALAS2, aminolevulinate δ synthase 2; BMP, bone morphogenetic protein; CUB domain, complement factor C1s/C1r, urchin embryonic growth factor and BMP domain; CMV, cytomegalovirus; DMEM, Dulbecco's modified Eagle's medium; EGFP, enhanced green fluorescent protein; FBS, fetal bovine serum; GAPDH, glyceraldehyde-3-phosphate dehydrogenase; HJV, haemojuvelin; IRIDA, iron-refractory iron-deficiency anaemia; LDLR domain, low-density-lipoprotein receptor class A domain; ORF, open reading frame; PIC, phosphoinositidase C; qRT-PCR, quantitative real-time PCR; SEA domain, sea urchin sperm protein, enteropeptidase and agrin domain; SELDI–TOF, surface-enhanced laser-desorption ionization–time-of-flight; SLC11A2, solute carrier family 11, member 2; SLC25A28, solute carrier family 25, member 28; TMPRSS6, transmembrane protease serine 6; cdTMPRSS6, catalytic domain of TMPRSS6; TTSP, type II transmembrane serine protease.

[1] These authors contributed equally to this work.

[2] To whom correspondence should be addressed (email martina.muckenthaler@med.uni-heidelberg.de).

as observed in IRIDA, inhibit intestinal iron absorption and macrophage iron release.

Under physiological conditions, TMPRSS6 down-regulates hepcidin levels by binding and proteolytically degrading the hepcidin activator and BMP co-receptor HJV (haemojuvelin), a protein mutated in hereditary haemochromatosis type 2 [13]. *TMPRSS6* mutations that decrease its proteolytic activity and prevent HJV cleavage cause increased hepcidin levels that impair iron release from the duodenal enterocytes and macrophages [13]. *TMPRSS6* mutations linked to IRIDA are detected throughout the *TMPRSS6* gene. These include missense, nonsense, frameshift and splice junction mutations [14]. Missense mutations are predominantly located in the CUB (G442R), LDLR (D521N, E522K) and protease (L674F and R774C) domains. Only a single mutation so far has been reported in the SEA domain (A118D) [15].

In the present paper, we report a novel homozygous missense mutation (c.422A>G) in exon 4 of *TMPRSS6* that replaces a tyrosine residue with a cysteine residue at amino acid 141. Interestingly, this mutation, located in the SEA domain, abolishes TMPRSS6 autocatalytic activation, causing an increase in hepcidin levels and the characteristic IRIDA phenotype. Together with a previous report [15], our finding suggests that the SEA domain plays an essential role in TMPRSS6 maturation and yields new insights into the proteolytic activation mechanism of this TTSP family member.

MATERIALS AND METHODS

Urinary hepcidin analysis

Hepcidin analysis was performed essentially as described previously [16]. Briefly, morning urine from the patient and from four age-and sex-matched healthy volunteers was centrifuged for 5 min at 3000 ***g***. After centrifugation, 7 μl of supernatant and 3 μl of 0.1M ammonium acetate buffer (pH 6) were mixed, incubated for 5 min at room temperature (22 °C) and directly applied to a pre-activated CM10 ProteinChip. Following 30 min of incubation in a humid chamber, the CM10 strip was washed three times with 30 mM ammonium acetate (pH 6) and air-dried. A total of 1 μl of SPA (sinapic acid) was added on to each spot, air-dried and reapplied. ProteinChips were read using a PBS IIc SELDI–TOF (surface-enhanced laser-desorption ionization–time-of-flight) mass spectrometer (BioRad Laboratories) pre-calibrated with a standard reference including synthetic hepcidin. Data acquisition parameters were set up to the following: high mass 50 000 Da, mass optimization from 1500 to 10 000 Da, laser intensity 180, detector sensitivity 9, mass deflector 1500 Da, two warming shots at an intensity of 185 (without warming shot collection), and acquisition of 50 shots every five positions from 27 to 87.

Data analysis was performed using the Ciphergen ProteinChip® Software version 3.2. Hepcidin levels, measured as arbitrary intensity units, were normalized against creatinine values obtained from the same samples (Analysezentrum, University Clinic of Heidelberg, Heidelberg, Germany). All samples were spotted and analysed in triplicate.

Patient clinical analysis

Informed consent was obtained from the parents of the patient and the healthy volunteers according to German law. Haematological parameters were measured at the Zentrum für Kinder und Jugendmedizin, St. Annastift, Ludwigshafen, Germany. The iron-related values (ferritin, transferrin, transferrin saturation, serum transferrin receptor, free serum iron, iron-binding capacity, zinc protoporphyrin, haptoglobin and erythropoietin) were measured at the Professor Seelig Laboratories, Karlsruhe, Germany. Patient DNA was extracted from peripheral blood by using the Qiagen DNeasy blood and tissue kit. Exons 1–18 of the *TMPRSS6* gene were amplified by PCR using Platinum Taq DNA Polymerase (Invitrogen) and primer pairs published previously [6]. Sequencing was performed by GATC Biotech. Chromatograms were visualized with FinchTV (Geospiza) and were analysed with SeqMan (DNAstar). *ALAS2* (aminolevulinate δ synthase 2; exons 1–10), *SLC25A28* (solute carrier family 25, member 28; exons 1–4), and *SLC11A2* (solute carrier family 11, member 2; exons 2–16) were PCR-amplified and sequenced at the Professor Seelig Laboratories, Karlsruhe, Germany.

Plasmids

The vector pcDNA3.1-TMPRSS6, expressing the wild-type *TMPRSS6* ORF (open reading frame) fused to the FLAG epitope at the C-terminus and the vector pcDNA3.1-mycHJV expressing human *HJV* cDNA in fusion with the Myc epitope were kindly provided by Dr Clara Camaschella (Division of Genetics and Cell Biology, San Raffaele Scientific Institute, Milan, Italy) [13].

The vector pcDNA3-HJV was created by cloning the PCR-amplified *HJV* ORF into the HindIII/EcoRI sites of the pcDNA3 vector. The *HJV* cDNA was PCR-amplified from HUH-7 cell-derived template cDNA by using the following primers: HJV-F: CCC**AAGCTT**ATGGGGGAGCCAGGCCA; and HJV-R: CCC**GAATTC**TTACTGAATGCAAAGCCACAGAAC (the recognition site of the restriction enzyme used to clone the PCR product is in bold).

The vector pcDNA3.1-TMPRSS6(Y141C), expressing the Y141C-mutated TMPRSS6 protein fused to the FLAG epitope at the C-terminus, was obtained using the Gene Tailor Site-Directed Mutagenesis System (Invitrogen) with the pcDNA3.1-TMPRSS6 as the template and the primers: Y141C-F: CTACAACTCCA-GCTCCGTCTGTTCCTTTGGGGA; and Y141C-R: AGACG-GAGCTGGAGTTGTAGTAAGTTCCCA.

The vector for the minigene system was generated by PCR amplification of 100 ng of patient genomic DNA using primers spanning from exons 3 to 5 within the *TMPRSS6* gene and Pfu Ultra DNA polymerase (Stratagene): ex3-F: AAA**GAATTC**GG-TACAAGGCGGAGGTGATG; and ex5-R: AAA**CTCGAG**CC-AGGATCACTAGGCCCTCG (the recognition site of the restriction enzyme used to clone the PCR product is in bold).

The PCR fragment was restriction-digested and cloned into the EcoRI/XhoI sites of the pcDNA3 vector (Invitrogen). The pEGFP-TMPRSS6 and pEGFP-TMPRSS6(Y141C) vectors were obtained by subcloning the coding sequence of *TMPRSS6* from the pcDNA3.1-TMPRSS6 and pcDNA3.1-TMPRSS6(Y141C) to pEGFP-n1 using the HindIII restriction sites.

All of the vectors were controlled via automatic sequencing performed by GATC Biotech.

Cell culture

The human hepatoma HuH-7 cell line and the human fibroblast HeLa cell line were cultured in high glucose DMEM (Dulbecco's modified Eagle's medium) with GlutaMAX (Invitrogen) supplemented with 10 % (v/v) heat-inactivated FBS (fetal bovine serum) (Invitrogen), 100 units/ml penicillin, 100 μg/ml streptomycin and 1 mM sodium pyruvate. The human hepatoma Hep3B cell line was cultured in EMEM (Eagle's minimum essential medium) supplemented with 10 % (v/v) FBS, 1 mM sodium pyruvate, 1 mM glutamine, 100 units/ml penicillin and 100 μg/ml streptomycin. Cells were maintained in a 5 % CO_2 atmosphere at 37 °C. Cell transfections were performed by using

the TransIT-LT1 Transfection Reagent (Mirus Bio), according to manufacturer's guidelines.

Microscopy

To analyse intracellular TMPRSS6 protein expression, 1.5×10^5 HeLa cells were plated on 420 mm^2 Lab-Tek chambered coverglass slides (Nunc) and transfected with pEGFP-TMPRSS6 or pEGFP-TMPRSS6(Y141C). After 48 h, the medium was replaced with DMEM complete medium without Phenol Red and the cells were analysed by live microscopy.

To analyse surface TMPRSS6 protein expression, 1.5×10^5 HeLa cells were plated on to a glass coverslip and transfected with pcDNA3.1-TMPRSS6 or pcDNA3.1-TMPRSS6(Y141C). After 48 h, the samples were fixed in 3 % PFA (paraformaldehyde), blocked with 1 % (w/v) BSA/0.3 M glycine in PBS, incubated overnight at 4 °C with an anti-FLAG (1:200 dilution; Sigma F3165) primary antibody and subsequently for 1 h with a FITC-conjugated anti-(mouse IgG) antibody (1:250 dilution; Sigma F5262). Cells were mounted on slides with Mowiol and analysed by microscopy. In both cases, samples were visualized using a PerkinElmer Improvision Ultraview VoX Spinning disc confocal microscope and were analysed with Improvision Volocity 5.3.1 and ImageJ 1.42q.

RNA isolation and qRT-PCR (quantitative real-time PCR)

Total RNA was isolated using the Qiagen RNAeasy kit according to the manufacturer's instruction. Total RNA (1 μg) was reverse-transcribed in a 25 μl reaction mixture using MMLV (Moloney-murine-leukaemia virus) reverse transcriptase (Fermentas) and random oligomers as primers. SYBR green real-time PCR was performed using the ABI StepONE Plus real-time PCR system (Applied Biosystems) using the following primers: hs_GAPDH-F, CATGAGAAGTATGACAACAGCCT; hs_GAPDH-R, AGTCCTTCCACGATACCAAAGT; hs_HAMP-F, CTCTGTTTTCCCACAACAGAC; and hs_HAMP-R, TAGGGGAAGTGGGTGTCTC.

Relative hepcidin mRNA expression was normalized to *GAPDH* (glyceraldehyde-3-phosphate dehydrogenase) mRNA. Results were calculated using the Pfaffl method [17].

Luciferase assay

Hep3B cells (9.5×10^5 cells/well) were plated on to a 12-well plate. After 24 h, the cells were transfected with 200 ng of pGL3-hepcidin(WT_2.7Kb) reporter vector containing 2.7 kb of the 5′-flanking genomic region of the human hepcidin gene plus its 5′-UTR (untranslated region), 10 ng of a control plasmid containing the *Renilla* gene under the control of the CMV (cytomegalovirus) promoter, 400 ng of pcDNA3-HJV vector and 200 ng of pcDNA3.1-TMPRSS6 or pcDNA3.1-TMPRSS6(Y141C). The next day, cells were lysed in passive lysis buffer (Promega), and cellular extracts were analysed for luciferase activity using the Dual Luciferase Reporter assay system (Promega) and a Centro LB 960 luminometer (Berthold Technologies).

Immunoprecipitation assay

HeLa cells (2×10^6) were transfected with 7.5 μg of pcDNA3.1-mycHJV and with 7.5 μg of pcDNA3.1-FLAG (mock), 7.5 μg of pcDNA3.1-TMPRSS6 or 7.5 μg of pcDNA3.1-TMPRSS6(Y141C). After 24 h, cells were lysed in NET buffer [50 mM Tris/HCl (pH 7.4), 150 mM NaCl, 5 mM EDTA, 1 % (v/v) Triton X-100] supplemented with sodium fluoride, PIC (phosphoinositidase C), PSMF and sodium orthovanadate. The lysate was incubated with 40 μl of pre-equilibrated anti-FLAG M2 affinity gel (Sigma A2220) for 4 h. After three washing steps in NET buffer, samples were eluted in Laemmli loading buffer [62.5 mM Tris/HCl (pH 6.8), 2 % (w/v) SDS, 10 % (v/v) glycerol, 0.1 % 2-mercaptoethanol and 0.0005 % Bromophenol Blue] and the eluted proteins were separated by SDS/PAGE (10 % gel) for Western blotting. Immunorecognition was performed by using an anti-FLAG (Sigma F7425) or an anti-c-Myc (Sigma C3956) polyclonal antibody.

Analysis of TMPRSS6 autocatalytic cleavage

HeLa cells (2.2×10^6) were seeded on to a 10-cm-diameter dish and transfected with 15 μg of pcDNA3.1-TMPRSS6, 15 μg of pcDNA3.1-TMPRSS6(Y141C) or 15 μg of pcDNA3.1-FLAG (mock) using the TransIT-LT1 Transfection Reagent (Mirus Bio) in DMEM complete medium. The next day, cells were washed with PBS and the medium was exchanged with serum-free OPTImem (Gibco) with or without 0.1 mM 2-mercaptoethanol to create a reduced environment. After 12 h, the supernatant was collected and concentrated using an Amicon Ultra 3K centrifugal filter (Millipore) (90 min at 4 °C at 4000 **g**). The cells were lysed in NET buffer supplemented with sodium fluoride, PIC, PSMF and sodium orthovanadate.

Protein concentrations were determined using the BCA (bicinchoninic acid) assay (Pierce). A portion (50 μg) of total protein extract or concentrated supernatant was separated by SDS/PAGE (10 % gel) and transferred on to a Protran BA83 nitrocellulose membrane. Monoclonal anti-tubulin (Sigma T5168), anti-FLAG (Sigma F7425), peroxidase-conjugated anti-(mouse IgG) (Sigma A9044) and peroxidase-conjugated anti-(rabbit IgG) (Sigma A0545) antibodies were used for immunorecognition.

Bioinformatic analysis

Sequence alignment of the SEA domain was performed by ClustalW (EBI; http://www.ebi.ac.uk/clustalw/). The sequences were retrieved from the GenBank® database using the following accession numbers: *Pan troglodites*, XR_024662; from the NCBI (National Center for Biotechnology Information) protein database using the following accession numbers: *Homo sapiens*, NP_705837; *Rattus norvegicus*, NP_001124028; *Mus musculus*, NP_082178; *Canis familiaris*, XP_531743; *Macaca mulatta*, XP_001085319 and *Monodelphis domestica*, XP_001376304; and from the ENSEMBL database with the following accession numbers: *Pongo pygmaeus*, ENSPPYP00000013149; *Cavia porcellus*, ENSCPOP00000004089; and *Ornithorhynchus anatinus*, ENSOANP00000021472.

The ribbon structure was obtained by using the crystal structure of the SEA domain of transmembrane protease from *M. Musculus* (PDB ID 2E7V) as the structural template and was readapted using the Swiss-Prot DeepView program version 4.0.1.

RESULTS

Patient clinical synopsis

Our patient is the second son of healthy non-consanguineous parents from Lebanon. Haematological disorders have not been reported in his family. In his second year of age, microcytic hypochromic anaemia was diagnosed. Subsequent iron supplementation did not improve his haematological parameters. As a 10-year-old boy, his family moved to Germany and he was

Table 1 Haematological parameters

An asterisk indicates pathological values. MCH, mean corpuscular haemoglobin content; MCV, mean corpuscular volume.

Parameter	Patient value	Normal range
Ferritin (ng/ml)	86	17–105
Transferrin (mg/dl)	262	210–315
Iron (μg/dl)*	12–18	92–184
Transferrin saturation (%)	3.3–4.8*	15–45
Soluble transferrin receptor (μg/dl)	4.77–5.03*	0.83–1.76
MCV (fl)*	59.8–62.5*	83–97
MCH (pg)*	16.4–17.7*	28–34
Haemoglobin (g/dl)*	7.9–9.4*	14–18
Zinc protoporphyrin (mmol/mol of haem)	378.2*	<40

referred to our Pediatric Haematology Department because of chronic weakness, occasional bone pain and extensive sleeping. His physical strength and fitness were normal, and he attended a regular school. He ate normal varied food and had normal appetite and stools. He had not suffered from infection or fever in recent months. Body weight was in the normal range between the tenth and 25th percentile, but his height had fallen to just below the third percentile. The laboratory parameters showed a persistent decrease in haemoglobin (7.9–9.4 g/dl), erythrocyte number [(4.82–5.5) $\times 10^6/\mu$l], mean corpuscolar volume (59.8–62.5 fl), and mean corpuscolar haemoglobin (16.4–17.7 pg). Reticulocytes and other blood cell counts were within the normal range, with the exception of thrombocytes which sometimes were increased with a maximum of 5.48 $\times 10^5/\mu$l. We found normal serum liver and renal parameters, including normal total protein and albumin. Analysis of iron metabolism parameters showed normal values for serum ferritin, transferrin and iron-binding capacity. By contrast, transferrin saturation (3.3–4.8 %) and serum iron levels (12–18 μg/dl) were pathologically low, whereas serum transferrin receptor levels (4.77–5.03 μg/dl) and zinc protoporphyrin in erythrocytes (332–378 μmol/mol of haemoglobulin; normal <40) were significantly increased. Bone marrow cytology showed normal blast numbers, erythropoiesis and megakaryopoiesis, both with discrete dysplastic features, and granulopoiesis. Iron staining discovered a clear lack of iron in macrophages. The bone marrow cytogenetic findings were normal. Pathologically low ^{59}Fe incorporation was observed from a scintigraphic examination, and this finding corresponded with the clinical observation of non-effective iron supplementation.

The haematological data collected from the proband are summarized in Table 1.

Urinary hepcidin levels are elevated in the IRIDA patient

Hypochromic microcytic anaemia with low transferrin saturation that cannot be treated by iron supplementation is a strong indication for IRIDA. Since this disorder is hallmarked by increased hepcidin expression, we analysed urinary hepcidin levels in the patient compared with four age-matched healthy male donors. The amount of the 25-amino-acid mature hepcidin peptide (Hamp-25) was analysed using SELDI–TOF MS and CM10 ProteinChip-arrays [16]. Hepcidin levels were normalized against creatinine (Figure 1). The data show severely increased (15-fold) hepcidin levels in the patient's urine, supporting the diagnosis of IRIDA.

c.442A>G, a novel mutation in exon 4 of *TMPRSS6*

To PCR-amplify all 18 *TMPRSS6* exons and exon/intron boundaries, PCR primers were designed within intronic

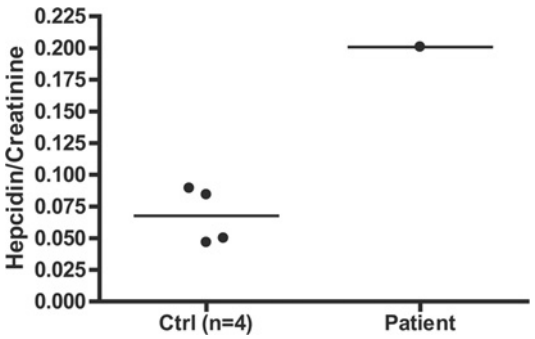

Figure 1 Elevated urinary hepcidin levels in the IRIDA patient

Urine was analysed from the IRIDA patient and four healthy age-matched male volunteers (Ctrl) by SELDI–TOF MS applying CM10 ProteinChips. Hepcidin arbitrary intensity units were normalized to creatinine.

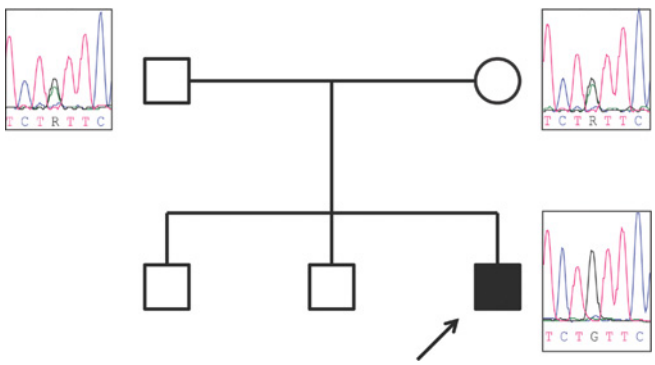

Figure 2 Family pedigree

Sequence analysis of the *TMPRSS6* gene indicates heterozygosity for the novel c.442A>G mutation in both parents, and homozygosity for the same mutation in the affected proband (marked by an arrow).

sequences. Sequence analysis of the PCR products failed to detect any *TMPRSS6* mutation associated previously with IRIDA. Instead, we identified a homozygous nucleotide exchange (c.442A>G) within exon 4 which, together with exons 3 and 5, constitutes the SEA domain. To exclude hemizygosity of the allele, we also sequenced exon 4 of *TMPRSS6* of both parents. As shown in Figure 2, a heterozygous c.442A>G base substitution was detected in both parents, clearly indicating that the mutation was homozygous in the patient.

Mutations in *ALAS2*, *SLC25A28* (*MFRN2*) and *SLC11A2* (*DMT1*) were excluded in previous analyses. Within the *SLC11A2* gene, a heterozygous SNP (single nucleotide polymorphism) in intron 5 (IVS5 + 60 C>T) was detected. Genetic haemoglobin analysis discovered a heterozygote $\alpha^{3.7}$-globin gene deletion which resulted in an α^+-thalassaemia trait.

TMPRSS6 c.422A>G does not affect splicing of exon 4

The novel c.442A>G mutation within exon 4 of the *TMPRSS6* gene is located ten nucleotides from the 3′-end of the exon and replaces the codon triplet TAT by TGT. This raises the possibility that the newly formed GT sequence could act as an aberrant 'splice donor' that may trigger incorrect splicing between the exons 4 and 5, leading to a premature termination of the TMPRSS6 protein.

Because TMPRSS6 expression is restricted to liver tissue [9], a splicing defect cannot be investigated by mRNA analysis of the patient's blood cells. We therefore designed a minigene that spans

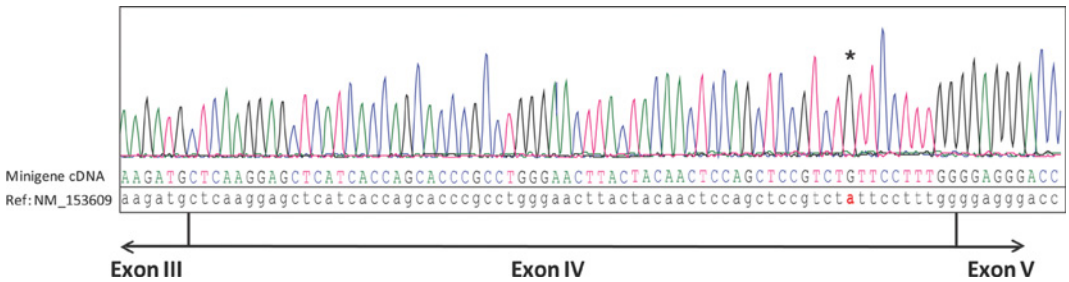

Figure 3 c.442A>G base substitution does not affect splicing

A minigene spanning exons 3 to 5 of the *TMPRSS6* gene was transfected in HeLa cells. Correct splicing between exons 4 and 5 was detected by sequence analysis of the resulting cDNA. The c.442A>G mutation is indicated by an asterisk. The sequence in capital letters indicates the sequence of the minigene. The sequence in lower case represents the sequence of the wild-type *TMPRSS6* cDNA (GenBank® accession number NM_153609).

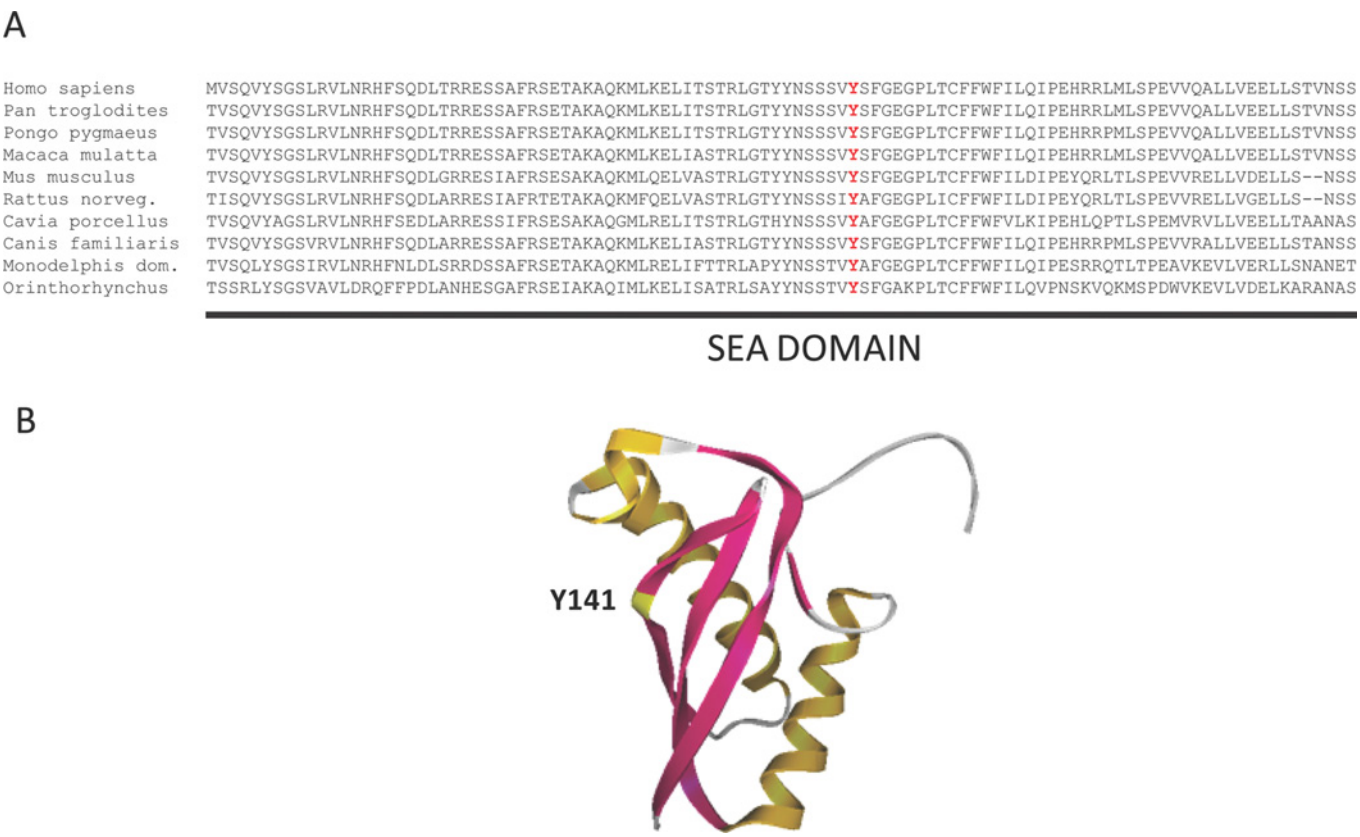

Figure 4 The tyrosine residue at position 141 is highly phylogenetically conserved

(**A**) Alignment of the TMPRSS6 SEA domain. Tyr^{141}, shown in bold red, is highly evolutionarily conserved. (**B**) Ribbon structure of the human SEA domain of TMPRSS6 generated by adaptation of the crystal structure of the SEA domain of the murine TMPRSS11d transmembrane protease (PDB ID 2E7V). The localization of Tyr^{141} within the second β-sheet of this domain is indicated.

exons 3 to 5 (including introns 3 and 4) of the *TMPRSS6* gene containing the c.442A>G mutation to transfect HeLa cells. As shown in Figure 3, this minigene construct is correctly spliced, suggesting that the c.442A>G mutation is unlikely to cause aberrant splicing.

TMPRSS6(Y141C) impairs TMPRSS6 maturation

The c.442A>G base substitution exchanges a tyrosine residue with a cysteine residue at amino acid 141 within the SEA domain of TMPRSS6. Phylogenetic sequence analysis of the TMPRSS6 protein indicates that amino acid residue 141 is highly conserved, suggesting that this tyrosine residue may be important for TMPRSS6 function (Figure 4A). Introduction of an additional cysteine residue within the second β-sheet of the SEA domain (Figure 4B) may interfere with secondary structure formation of TMPRSS6, a protein that already contains 37 cysteine residues. We therefore next assessed whether the TMPRSS6(Y141C) mutation causes protein mislocalization. TMPRSS6(Y141C) or TMPRSS6 protein fused to EGFP (enhanced green fluorescent protein) was expressed in HeLa cells and the fluorescent signal was analysed by confocal

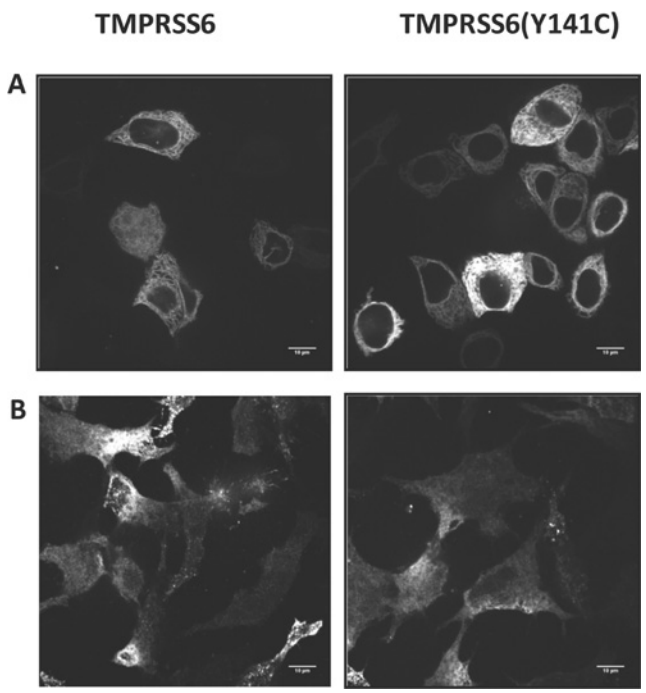

Figure 5 TMPRSS6 and TMPRSS6(Y141C) localize to similar subcellular regions

(**A**) Localization of transfected TMPRSS6–EGFP and TMPRSS6(Y141C)–EGFP in HeLa cells by live confocal microscopy. (**B**) Cell-surface expression of TMPRSS6–FLAG and TMPRSS6(Y141C)–FLAG in transiently transfected HeLa cells. Cells were fixed without permeabilization, and membrane proteins were detected using an anti-FLAG antibody. Signal detection was by confocal microscopy.

microscopy. As shown in Figure 5(A), both the overexpressed wild-type and mutant TMPRSS6 proteins localize predominantly in intracellular compartments (e.g. the endoplasmic reticulum). To assess membrane localization of TMPRSS6, HeLa cells were transfected with TMPRSS6 or TMPRSS6(Y141C), both C-terminally fused with a FLAG epitope that is predicted to be located in the extracellular space. The cells were analysed by immunocytochemistry using primary anti-FLAG and secondary FITC-conjugated antibodies on fixed non-permeabilized cells. As shown in Figure 5(B), both the TMPRSS6 and TMPRSS6(Y141C) proteins localize to the cell surface, suggesting that faulty processing and localization of the TMPRSS6 mutant protein does not explain IRIDA in the patient.

TMPRSS6 was shown to control hepcidin mRNA expression by binding and proteolytically cleaving HJV [18]. To assess whether amino acid residue 141 of TMPRSS6 is critical for binding HJV we next transfected HeLa cells with a Myc-tagged HJV fusion construct alone or together with plasmids coding for TMPRSS6 or TMPRSS6(Y141C) proteins both tagged with a FLAG epitope. Immunoprecipitation of TMPRSS6 or TMPRSS6(Y141C) using anti-FLAG antibodies both detects HJV protein at the expected molecular mass of 55 kDa (Figure 6A, lanes 2 and 3). No signal was detected in the sample transfected with HJV and a control vector (Figure 6A, lane 1). This experiment demonstrates that the Y141C mutation does not affect binding to HJV.

TMPRSS6, like other serine proteases, is auto-activated by proteolytic cleavage within a RIVGG motif at its pro-domain/catalytic domain junction site. Once cleaved, the 30 kDa catalytic domain remains attached to the rest of the protein via a disulfide bridge. HeLa cells were transfected with a control plasmid or with plasmids coding for TMPRSS6 or TMPRSS6(Y141C). Subsequently, both the cell lysates as well as the concentrated medium supernatant were analysed for TMPRSS6 expression by Western blotting. Interestingly, only conditioned medium from cells transfected with the TMPRSS6 plasmid revealed a TMPRSS6 protein fragment of approx. 30 kDa, which corresponds to the expected mass of cdTMPRSS6 (catalytic domain of TMPRSS6) (Figure 6B, lane 2). A similar fragment failed to be detected in cells transfected with the TMPRSS6(Y141C) (Figure 6B, lane 3) or control vectors (Figure 6B, lane 1), despite efficient expression of the TMPRSS6(Y141C) protein as detected in the cell lysate (Figure 6B, middle panel). Analysis of equal protein amounts was assured by detection of tubulin (Figure 6B, lower panel).

A lack of cdTMPRSS6 in the conditioned medium of TMPRSS6(Y141C)-transfected cells may either indicate a lack of proteolytic auto-activation of the mutated protein or increased binding stability of the catalytic domain to the rest of the protein, due to the formation of an extra disulfide bond in the Y141C-mutated protein.

In an attempt to distinguish between these two possibilities, we repeated the experiment but added the reducing agent 2-mercaptoethanol (0.1 mM) to the cell culture medium. As shown in Figure 6(C) (upper panel, lanes 3 and 4), HeLa cells transfected with TMPRSS6(Y141C) failed to release cdTMPRSS6 into the medium, both under normal and reducing conditions. By contrast, cdTMPRSS6 was readily detected under both conditions in cells transfected with the wild-type construct (Figure 6C). Efficient protein expression of TMPRSS6 and the mutant form were found in the cell lysate (Figure 6C, lower panel).

Taken together these data support the interpretation that TMPRSS6(Y141C) fails to be auto-activated by proteolytic cleavage.

TMPRSS6(Y141C) overexpression increases hepcidin mRNA expression

TMPRSS6(Y141C) overexpression leads to the synthesis of an inactive form of TMPRSS6. To assess whether this defect affects hepcidin mRNA expression, we next transfected the human hepatoma cell line Hep3B with a firefly luciferase reporter vector under the control of the full-length hepcidin promoter, together with expression vectors coding for HJV and TMPRSS6 or TMPRSS6(Y141C) proteins. Firefly luciferase activity was normalized with *Renilla* luciferase under the control of a constitutive CMV promoter.

As expected, transfection of the HJV expression vector resulted in a 3.5-fold increase in luciferase activity. Co-transfection with TMPRSS6 completely abolished this effect. Importantly, co-transfection of TMPRSS6(Y141C) only slightly attenuated the HJV-controlled hepcidin response, resulting in a 2-fold activation of the hepcidin promoter (Figure 7A). Similar findings were obtained analysing endogeneous hepcidin mRNA levels (Figure 7B), suggesting that the amino acid substitution at position 141 is sufficient to inhibit HJV-controlled hepcidin activation and, thus, probably explains the IRIDA phenotype.

DISCUSSION

In the present paper, we report the clinical case of a 10-year-old boy with IRIDA hallmarked by microcytic hypochromic anaemia that could not be resolved by iron administration. Iron treatment was probably ineffective as a consequence of high hepcidin levels in the blood, reflected by increased urinary hepcidin excretion (Figure 1), which blocks duodenal iron uptake and macrophage iron release [19]. Sequence analysis

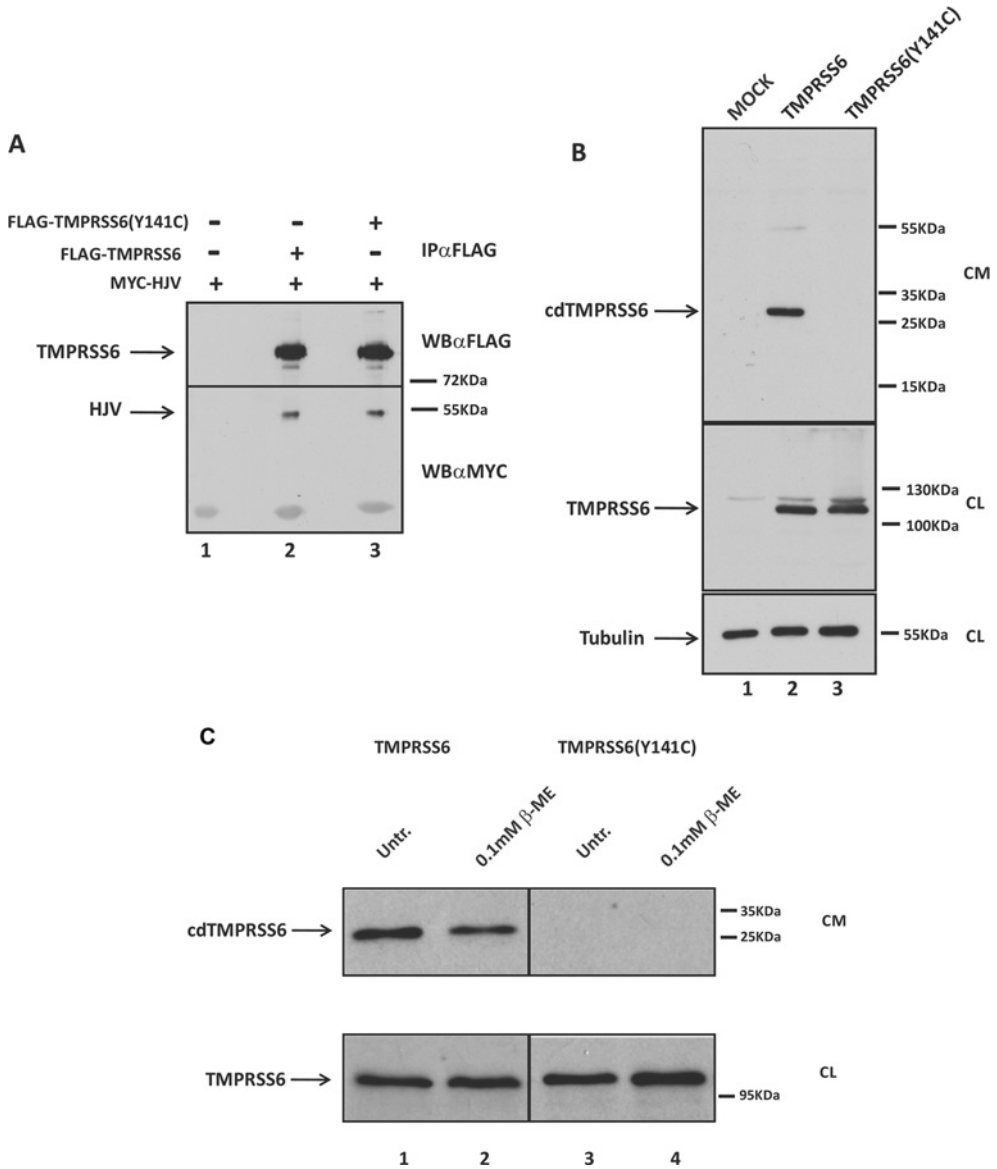

Figure 6 TMPRSS6(Y141C) binds HJV, but fails to auto-catalytically activate itself

(**A**) HeLa cells were transfected with plasmids expressing HJV-Myc or pcDNA3.1-FLAG (mock), TMPRSS6-FLAG or TMPRSS6(Y141C)-FLAG as indicated. After TMPRSS6 immunoprecipitation using an anti-Flag antibody (IPαFLAG), TMPRSS6 and the TMPRSS6-bound HJV were immunorecognized by Western blotting using an anti-FLAG antibody (WBαFLAG) or an anti-Myc antibody (WBαMyc) respectively. (**B**) HeLa cells were transfected with pcDNA3.1-FLAG (mock), TMPRSS6-FLAG or TMPRSS6(Y141C)-FLAG. After 24 in serum-free medium, the conditioned medium (CM) was collected, concentrated and analysed for the presence of the proteolytic TMPRSS6 fragments by Western blotting. (**C**) HeLa cells were transfected with TMPRSS6-FLAG or TMPRSS6(Y141C)-FLAG, washed and incubated with serum-free OPTImem (Gibco) with or without 0.1 mM 2-mercaptoethanol (β-ME) for 12 h. The conditioned medium was collected, concentrated and analysed by Western blotting for cdTMPRSS6. Effective TMPRSS6 transfection was assessed in the cell lysate (CL).

detected a homozygous mutation (c.422A>G) within exon 4 of the *TMPRSS6* gene (Figure 2). We initially hypothesized that replacing the codon triplet TAT with TGT may generate an additional 'splice donor' sequence. However, a transfected minigene containing the mutation was accurately spliced between exon 4 and 5 (Figure 3), suggesting that an amino acid replacement of a tyrosine residue by a cysteine residue at amino acid 141 may affect TMPRSS6 function. The mutation is located within the SEA domain of TMPRSS6, which is predicted to be localized within the extracellular part of the TMPRSS6 protein. An SEA domain is also present in enteropeptidase, another TTSP family member, in all of the HAT/DESC (human airway trypsin-like protease/differentially expressed in squamous cell carcinoma) subfamily proteins and in the closely related matriptase and matriptase-3 [20]. The biological role of this domain remains to be determined. In some proteins, the SEA domain is subject to autoproteolysis causing the production of a soluble form of the protein that is released from the cell surface. Such an autoproteolytic event can be accelerated by conformational stress within the SEA domain itself [21]. Cleavage occurs between the glycine and serine residues within a conserved GSVVV (mucin), GSVIV (enteropeptidase) or GSVIA (matriptase) motif [21–23]. It is not yet clear whether the SEA domain of the human TMPRSS6 is also subject to autoproteolysis. Analysis of the primary amino acid sequence failed to detect a common cleavage motif identifying only a putative GSLRV motif.

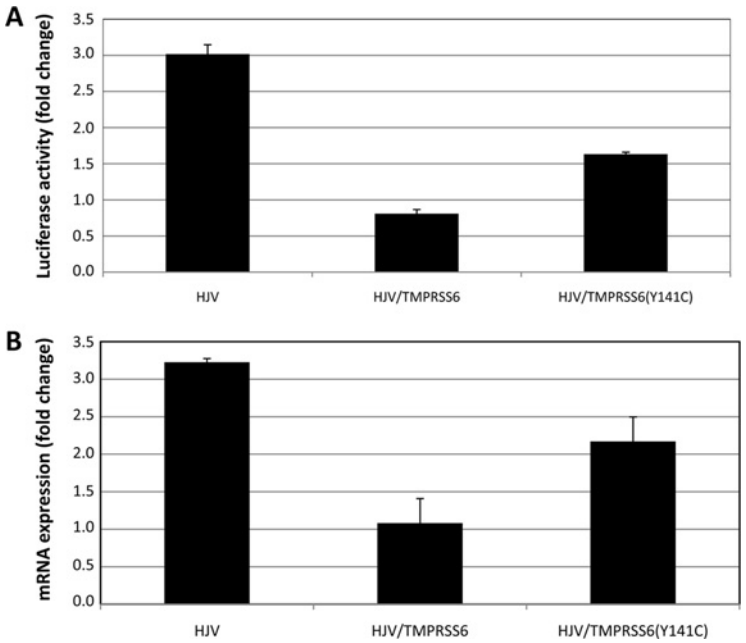

Figure 7 TMPRSS6(Y141C) expression fails to efficiently suppress hepcidin promoter activity

(**A**) Luciferase assay. The reporter plasmid pGL3-hepcidin(WT_2.7kb) was transfected with either HJV alone or together with TMPRSS6 or TMPRSS6(Y141C) in Hep3B cells. At 24 h later, luciferase activity was measured and normalized against *Renilla* luciferase. Results are mean ± S.D. fold changes of transfected cells compared with cells transfected with the reporter construct (WT_2.7kb) only. (**B**) qRT-PCR assay. Hep3B cells were transfected with either HJV alone or together with TMPRSS6 or TMPRSS6(Y141C). At 24 h later, total RNA was extracted. Hepcidin mRNA expression was analysed by qRT-PCR and was normalized to GAPDH. Results are mean ± S.D. fold changes.

The TMPRSS6(Y141C) protein localizes to similar subcellular regions as the wild-type TMPRSS6 protein (Figure 5), suggesting that selective retention of TMPRSS6(Y141C) protein within the cytoplasm does not occur. Immunoblotting of medium supernatant of TMPRSS6(Y141C)- and TMPRSS6-transfected cells failed to detect the entire extracellular domain of the TMPRSS6 protein as a consequence of cleavage within the SEA domain, in contrast with findings by Ramsay and co-workers [10], who detected fragments of the appropriate size in both wild-type and mutant TMPRSS6 proteins.

So far, it is not clear which protein domain of TMPRSS6 binds to HJV and *vice versa*. In the present report, we show that the TMPRSS6(Y141C) mutation does not affect co-immunoprecipitation with HJV, suggesting that the interaction domain may be localized within other domains of TMPRSS6.

Finally, we show that the Y141C amino acid substitution affects the maturation of the TMPRSS6 protein. TMPRSS6 is initially synthesized as an inactive proenzyme that, upon auto-activation, cleaves the C-terminal catalytic domain within the RIVGG consensus sequence. The cleaved domain remains attached to the rest of the protein via a disulfide bond. Western blot analysis (under reducing conditions) of tissue culture medium from cells transfected with TMPRSS6 revealed a 30 kDa fragment that corresponds in size to the activated cdTMPRSS6 protein. In addition, we detected a minor 60 kDa fragment that has been proposed previously to represent a dimeric form of cdTMPRSS6 [18]. Interestingly, both the 30 and 60 kDa fragments were undetectable in TMPRSS6(Y141C)-transfected cells. It is unlikely that the additional cysteine residue in TMPRSS6(Y141C) may have stabilized the interaction between cdTMPRSS6 and the rest of the protein, because the addition of 2-mercaptoethanol to the cell culture medium did not result in the detection of cdTMPRSS6 upon expression of TMPRSS6(Y141C) (Figure 6C). Our present data thus suggest that the tyrosine residue at amino acid 141 is probably required for TMPRSS6 autocatalytic cleavage. TMPRSS6 auto-activation is critical for protein function because transfection of TMPRSS6(Y141C) fails to attenuate hepcidin promoter activity (Figure 7). As a consequence, hepcidin levels will be increased (Figure 1) and IRIDA will develop.

Interestingly, an additional mutation in the SEA domain (A118D) was recently shown to be critical for TMPRSS6 auto-activation [15]. It is thus intriguing to speculate that the SEA domain could act as a scaffold structure that maintains TMPRSS6 folding in order for auto-activation to occur. Replacement of a tyrosine residue with an additional cysteine residue within the second β-sheet of the SEA domain (Figure 4B) may interfere with the formation of disulfide bridges within TMPRSS6, a protein that already contains 37 cysteine residues. Alternatively, the mutation could affect N-linked glycosylation of the SEA domain that may affect protein stability.

Together with other findings, our present results suggest that unprocessed TMPRSS6(Y141C) still reaches the cell surface and interacts with HJV, but fails to cleave HJV. As a consequence, the BMP/SMAD4 signalling pathway is hyperactive resulting in excess hepcidin transcription. Functional characterization of the TMPRSS6(Y141C) thus gives novel insight into understanding TMPRSS6 function and the pathogenesis of IRIDA.

AUTHOR CONTRIBUTION

Sandro Altamura performed and analysed the experiments, and wrote the first draft of the paper. Flavia D'Alessio performed the luciferase and qRT-PCR experiments. Barbara Selle followed the patient, performed the diagnosis and provided the clinical data. Martina Muckenthaler supervised the research and wrote the manuscript.

ACKNOWLEDGEMENTS

We thank M. Hentze for helpful discussions.

FUNDING

This study is supported by eRARE-BMBF (HMA-IRON) to M.U.M. S.A. is funded by the Medical Faculty of Heidelberg.

REFERENCES

1 Buchanan, G. R. and Sheehan, R. G. (1981) Malabsorption and defective utilization of iron in three siblings. J. Pediatr. **98**, 723–728
2 Melis, M. A., Cau, M., Congiu, R., Sole, G., Barella, S., Cao, A., Westerman, M., Cazzola, M. and Galanello, R. (2008) A mutation in the TMPRSS6 gene, encoding a transmembrane serine protease that suppresses hepcidin production, in familial iron deficiency anemia refractory to oral iron. Haematologica **93**, 1473–1479
3 Andrews, N. C. (1997) Iron deficiency: lessons from anemic mice. Yale J. Biol. Med. **70**, 219–226
4 Pearson, H. A. and Lukens, J. N. (1999) Ferrokinetics in the syndrome of familial hypoferremic microcytic anemia with iron malabsorption. J. Pediatr. Hematol. Oncol. **21**, 412–417
5 Brown, A. C., Lutton, J. D., Pearson, H. A., Nelson, J. C., Levere, R. D. and Abraham, N. G. (1988) Heme metabolism and in vitro erythropoiesis in anemia associated with hypochromic microcytosis. Am. J. Hematol. **27**, 1–6
6 Finberg, K. E., Heeney, M. M., Campagna, D. R., Aydinok, Y., Pearson, H. A., Hartman, K. R., Mayo, M. M., Samuel, S. M., Strouse, J. J., Markianos, K. et al. (2008) Mutations in TMPRSS6 cause iron-refractory iron deficiency anemia (IRIDA). Nat. Genet. **40**, 569–571
7 Folgueras, A. R., de Lara, F. M., Pendas, A. M., Garabaya, C., Rodriguez, F., Astudillo, A., Bernal, T., Cabanillas, R., Lopez-Otin, C. and Velasco, G. (2008) Membrane-bound serine protease matriptase-2 (Tmprss6) is an essential regulator of iron homeostasis. Blood **112**, 2539–2545
8 Du, X., She, E., Gelbart, T., Truksa, J., Lee, P., Xia, Y., Khovananth, K., Mudd, S., Mann, N., Moresco, E. M., Beutler, E. and Beutler, B. (2008) The serine protease TMPRSS6 is required to sense iron deficiency. Science **320**, 1088–1092
9 Velasco, G., Cal, S., Quesada, V., Sanchez, L. M. and Lopez-Otin, C. (2002) Matriptase-2, a membrane-bound mosaic serine proteinase predominantly expressed in human liver and showing degrading activity against extracellular matrix proteins. J. Biol. Chem. **277**, 37637–37646
10 Ramsay, A. J., Reid, J. C., Velasco, G., Quigley, J. P. and Hooper, J. D. (2008) The type II transmembrane serine protease matriptase-2–identification, structural features, enzymology, expression pattern and potential roles. Front. Biosci. **13**, 569–579
11 Hooper, J. D., Campagnolo, L., Goodarzi, G., Truong, T. N., Stuhlmann, H. and Quigley, J. P. (2003) Mouse matriptase-2: identification, characterization and comparative mRNA expression analysis with mouse hepsin in adult and embryonic tissues. Biochem. J. **373**, 689–702
12 Nemeth, E., Tuttle, M. S., Powelson, J., Vaughn, M. B., Donovan, A., Ward, D. M., Ganz, T. and Kaplan, J. (2004) Hepcidin regulates cellular iron efflux by binding to ferroportin and inducing its internalization. Science **306**, 2090–2093
13 Silvestri, L., Guillem, F., Pagani, A., Nai, A., Oudin, C., Silva, M., Toutain, F., Kannengiesser, C., Beaumont, C., Camaschella, C. and Grandchamp, B. (2009) Molecular mechanisms of the defective hepcidin inhibition in TMPRSS6 mutations associated with iron-refractory iron deficiency anemia. Blood **113**, 5605–5608
14 Lee, P. (2009) Role of matriptase-2 (TMPRSS6) in iron metabolism. Acta Haematol. **122**, 87–96
15 Ramsay, A. J., Quesada, V., Sanchez, M., Garabaya, C., Sarda, M. P., Baiget, M., Remacha, A., Velasco, G. and Lopez-Otin, C. (2009) Matriptase-2 mutations in iron-refractory iron deficiency anemia patients provide new insights into protease activation mechanisms. Hum. Mol. Genet. **18**, 3673–3683
16 Altamura, S., Kiss, J., Blattmann, C., Gilles, W. and Muckenthaler, M. U. (2009) SELDI-TOF MS detection of urinary hepcidin. Biochimie **91**, 1335–1338
17 Pfaffl, M. W. (2001) A new mathematical model for relative quantification in real-time RT-PCR. Nucleic Acids Res. **29**, 2002–2007
18 Silvestri, L., Pagani, A., Nai, A., De Domenico, I., Kaplan, J. and Camaschella, C. (2008) The serine protease matriptase-2 (TMPRSS6) inhibits hepcidin activation by cleaving membrane hemojuvelin. Cell Metab. **8**, 502–511
19 Muckenthaler, M. U. (2008) Fine tuning of hepcidin expression by positive and negative regulators. Cell Metab. **8**, 1–3
20 Bugge, T. H., Antalis, T. M. and Wu, Q. (2009) Type II transmembrane serine proteases. J. Biol. Chem. **284**, 23177–23181
21 Macao, B., Johansson, D. G., Hansson, G. C. and Hard, T. (2006) Autoproteolysis coupled to protein folding in the SEA domain of the membrane-bound MUC1 mucin. Nat. Struct. Mol. Biol. **13**, 71–76
22 Matsushima, M., Ichinose, M., Yahagi, N., Kakei, N., Tsukada, S., Miki, K., Kurokawa, K., Tashiro, K., Shiokawa, K., Shinomiya, K. et al. (1994) Structural characterization of porcine enteropeptidase. J. Biol. Chem. **269**, 19976–19982
23 Cho, E. G., Kim, M. G., Kim, C., Kim, S. R., Seong, I. S., Chung, C., Schwartz, R. H. and Park, D. (2001) N-terminal processing is essential for release of epithin, a mouse type II membrane serine protease. J. Biol. Chem. **276**, 44581–44589

Received 4 May 2010/3 August 2010; accepted 12 August 2010
Published as BJ Immediate Publication 12 August 2010, doi:10.1042/BJ20100668